White Dwarfs in Dwarf Spheroidal Galaxies: A New Class of Compact-Dark-Matter Detectors

Juri Smirnov[1,2,*] Ariel Goobar[2,†] Tim Linden[2,‡] and Edvard Mörtsell[2,§]

[1]*Department of Mathematical Sciences, University of Liverpool, Liverpool L69 7ZL, United Kingdom*
[2]*The Oskar Klein Centre, Department of Physics, Stockholm University, AlbaNova, SE-10691 Stockholm, Sweden*

Recent surveys have discovered a population of faint supernovae, known as Ca-rich gap transients, inferred to originate from explosive ignitions of white dwarfs. In addition to their unique spectra and luminosities, these supernovae have an unusual spatial distribution and are predominantly found at large distances from their presumed host galaxies. We show that the locations of Ca-rich gap transients are well matched to the distribution of dwarf spheroidal galaxies surrounding large galaxies, in a scenario where dark matter interactions induce thermonuclear explosions among low-mass white dwarfs that may be otherwise difficult to ignite with standard stellar or binary evolution mechanisms. A plausible candidate to explain the observed event rate are primordial black holes with masses above 10^{21} grams.

Recent surveys have uncovered a new population of supernovae (SN) with peculiar properties [1,2], called Ca-Rich gap transients. Compared to standard Type Ia SN, which trace stellar density, Ca-rich events are located at a larger offset from the center of their host galaxies. Additionally, spectral observations seem to indicate that they originate from white dwarfs with masses well below the Chandrasekhar limit, near $\sim 0.6 M_{\odot}$ [3]. Finally, these events predominantly occur in old systems, such as elliptical galaxies.

White dwarfs (WDs) are essentially nuclear bombs in space—waiting to be ignited by sufficient energy injection. We propose that Ca-Rich transients are naturally explained in a scenario where WDs can be ignited by interactions with compact dark matter (DM) relics, which appear in many scenarios [4–13]. The ignition mechanism has been proposed in Refs. [14,15], and further studied in Ref. [16]. For a summary, see the Supplemental Material [17].

We show that this scenario naturally explains the spatial distribution of Ca-rich transients for two reasons. First, the abundance of low-mass WDs is about an order of magnitude larger in systems older than eight Gyrs, compared to systems younger than three Gyrs. Second, the event rate is dominated by ignition in dwarf spheroidal galaxies (dSphs) surrounding the host galaxy, which leads to clustering at large radii.

While many models include primordial black holes (PBH) as a fraction of the DM, the observed Ca-Rich transient event rate points towards the existence of asteroid mass PBHs that lie within reach of current or near-future microlensing surveys [18,19]. Furthermore, follow-up localization of the Ca-Rich events would be expected to be correlated with dSphs surrounding distant galaxies. Thus, we find that supernovae triggered by PBH impacts could serve as beacons for a new class of DM searches.

Figure 1 shows the cumulative Type Ia SN (SNIa) event rate normalized to the total event rate of each class. The x axis shows the position of the events, normalized to the half-light radii of the host galaxies, as determined by Ref. [2]. For standard SNIa, observations closely follow the stellar distribution, matching expectations for events driven by binary interactions. Ca-rich transients, however, have a significantly extended profile that does not match the stellar distribution. Intriguingly, the galactocentric distance profile of these SNe is well-fit by the modeled distribution of DM-WD interactions, including a significant contribution from dSphs that surround the host galaxies. This close spatial match, in addition to the unique chemical properties and atypical progenitors of Ca-rich transients, motivates an interpretation where these events may be driven by DM-WD interactions. Note that the uncertainties on the event rate in individual bins of Ca-rich transients at low radii are $\sim 20\%$, such that the apparent over-prediction of the events at radii below $R_{1/2} \sim 2$ is not statistically significant. Moreover, a selection effect is expected where very faint SNe are missed if they occur at the bright cores of galaxies.

Ca-rich gap transients.—Ca-rich transients are identified based on their spectral and morphological properties [1]. They are predominantly found in the outskirts of elliptical galaxies, with offsets from the presumed host that can reach ~ 100 kpc [2], in contrast to the radial stellar density
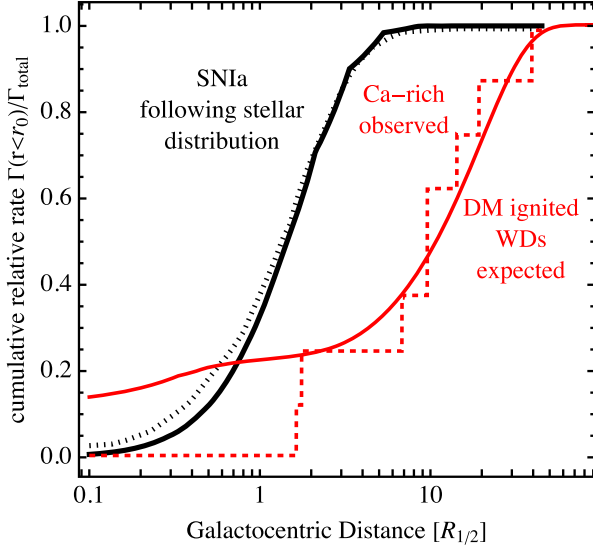
FIG. 1. Cumulative radial distributions of standard Type Ia SNe (black dashed) and Ca-rich gap transients (red dashed) within their host galaxies [2] normalized to the total respective event rates. Results are compared to the spatial distribution of galactic stars (black solid) and the expected distribution of DM-WD interactions (red solid). Ca-rich transients closely fit the morphology of DM-WD interactions.

profiles of galaxies as well as both Type Ia and core-collapse SN. Ca-rich transients also differ from other SN in that they evolve faster to the nebular emission phase, where they become "Ca-rich," as defined by the integrated flux ratio in [Ca II] ($\lambda\lambda$7291, 7324) over [O I] ($\lambda\lambda$6300, 6364) [20].

Because they are found in old environments and lack hydrogen spectral features, Ca-rich transients are hypothesized to stem from low-mass WDs [3]. However, compared to "normal" Type Ia SNe, which are typically modeled as the explosion of a WD in a binary system, Ca-rich transients have much lower peak brightness, occupying a "gap" between novae and supernovae. Additionally, their narrow lightcurves indicate lower-mass ($\sim 0.6 M_\odot$, or even lower [21]) WD progenitors, compared to standard binary models. Because of their faintness, current SN surveys have only found these transients in a relatively small volume compared to other SNe. Hence, the Ca-rich transient sample is small. After correcting for selection effects, their calculated rate is $0.13^{+0.06}_{-0.04} \times$ the Type Ia SN rate, or $3.19^{+1.45}_{-0.96} \times 10^{-6}$ Mpc^{-3} yr^{-1} [22].

Given the difficulty in modeling these SNe using stellar explosions in binary systems; see, e.g. [23,24] for recent ideas, we consider the possibility that Ca-rich transients are the result of the explosion of a *single* white dwarf (WD), where the thermonuclear runaway is triggered by the passage of DM. To explore this hypothesis, we investigate the expected galactocentric distances of such explosions, taking into account the spatial and velocity distributions of WDS and DM.

Dark matter induced white dwarf ignition.—We can express the WD explosion rate as

$$\Gamma_{\text{ign}} = \phi_{\text{DM}} f_{\text{ign}} = \pi R^2 \frac{\rho_{\text{DM}}}{m_{\text{DM}}} v_0 \left(1 + \frac{3}{2} \frac{v_{\text{esc}}^2}{v_{\text{DM}}^2}\right) f_{\text{ign}}, \quad (1)$$

where $v_0 = \sqrt{8/(3\pi)} v_{\text{DM}}$, v_{DM} is the DM velocity dispersion at the considered position, ϕ_{DM} the DM density, R the WD radius, and v_{esc} the WD escape velocity. The factor f_{ign} encodes the probability of a PBH igniting the WD during transit. We will model this probability as a step function in the PBH mass, based on the parametrization discussed in Supplemental Material I [17], which includes Refs. [25–30]. Note that a detailed simulation would be required to obtain exact values for f_{ign}, as discussed in Ref. [16]. In particular, Ref. [16] shows that given the uncertainty on the ignition probability, WD observations currently place no bounds on PBHs. A signal detection, however, would favor a given ignition scenario.

We obtain the DM-induced ignition rate by the integral

$$\Gamma_\Omega = \int_\Omega dV \Gamma_{\text{ign}} n_{\text{WD}}, \quad (2)$$

where n_{WD} is the WD number density and Ω is the region of interest. We use this formalism to calculate the induced WD ignition rates in several environments.

Milky Way as a template.—Most Ca-rich transients have been found near galaxies with masses comparable to the Milky Way. This makes it reasonable to use the Milky Way as a "template" to estimate the distribution of Ca-rich transients around galaxies. We will define these analog galaxies as "Milky Way equivalent galaxies" (MWEGs) [31].

Determining the radial distribution of Ca-rich transients in an MWEG requires models for the Milky Way DM density, stellar density, and star-formation history. For the DM density, we utilize a generalized Navarro-Frenk-White (gNFW) profile [32]:

$$\rho_{\text{DM}}(r; \gamma, r_s, \rho_0) = \rho_0 \left(\frac{R_0}{r}\right)^\gamma \left(\frac{r_s + R_0}{r_s + r}\right)^{3-\gamma}, \quad (3)$$

where $\rho_0 = 0.42$ GeV cm^{-3} [33] is the DM density at the solar position $R_0 = 8.15$ kpc [34]. We consider a cuspy NFW profile with $r_s = 10.4$ kpc and $\gamma = 1$, and a cored profile with $r_s = 6.4$ kpc and $\gamma = 0.01$ representing values that are consistent with studies of the Milky Way DM density for different baryonic models [35]. The DM dispersion velocity includes significant baryonic contributions, and we utilize the fitting results of Ref. [36].

Constructing complete observations of Milky Way WDs is difficult due to their low luminosity. Thus, we model the Milky Way WD population by examining the density distribution and star-formation history of their progenitors. We take the stellar density from the SDSS Milky Way

tomography [37], and calculate the star-formation history from the fitting function [38]:

$$\dot{\rho}_{\text{star}} = \frac{h(a + bz)}{1 + (z/c)^d},\qquad(4)$$

where $h = 0.7$, and the coefficients have been fitted to $a = 0.017$, $b = 0.13$, $c = 3.3$, and $d = 5.3$.

The redshift-time relation is calculated using

$$\tau(z) = H_0^{-1} \int_z^\infty \frac{dx}{(1 + x)\sqrt{\mathcal{E}(x)}},\quad \text{with}$$

$$E(z) = \Omega_\Lambda + \Omega_M (1 + z)^3 + \Omega_R (1 + z)^4,\qquad(5)$$

for which we use cosmological values from [39]. We use the Kroupa initial mass function [40] for the stellar distribution:

$$\zeta_{\text{MW}} = \frac{dN_{\text{star}}}{dM}$$

$$= \frac{\kappa}{M^\alpha} \begin{cases} \kappa = 0.07, \alpha = 2.3, & \text{if } \frac{M}{M_\odot} \geq 0.5, \\ \kappa = 0.14, \alpha = 1.3, & \text{if } 0.5 > \frac{M}{M_\odot} \geq 0.08, \\ \kappa = 1.78, \alpha = 0.3, & \text{if } \frac{M}{M_\odot} < 0.08. \end{cases}$$

$$(6)$$

The WD mass upper limit of $8M_\odot$ stems from the lower-bound for electron-capture SN [41], while the minimum WD mass depends on the stellar age, as

$$\frac{M_{\text{min}}}{M_\odot} = \min\left[\left(1 - \frac{\tau_{\text{birth}}}{\tau_{\text{max}}}\right)^{-2/5}, 8\right],\qquad(7)$$

where $\tau_{\text{max}} \approx 10$ Gyr. Combined, we find a WD fraction:

$$f_{\text{WD}}^{\text{MW}} = \frac{\int_0^{\tau_{\text{max}}} d\tau \dot{\rho}_{\text{star}} \int_{M_{\text{min}}(\tau)}^{M_{\text{max}}} dM \zeta_{\text{MW}}}{\int_0^{\tau_{\text{max}}} d\tau \dot{\rho}_{\text{star}} \int_0^{100 M_\odot} dM \zeta_{\text{MW}}} \approx 0.035.\quad(8)$$

We have confirmed that this number does not strongly depend on the exact form of the stellar birth rate, and is a robust estimate for the WD fraction of the MW.

Assuming that every DM transit triggers a WD explosion, we obtain a WD ignition rate of

$$R_{\text{MW}} = (5 \pm 3) \times 10^{-4}\left(\frac{10^{24}\,\text{g}}{M_{\text{PBH}}}\right)\,\text{yr}^{-1}.\qquad(9)$$

Since this calculation includes significant uncertainties, it is best viewed as an order-of-magnitude estimate. Note that the galaxies we consider are located at small redshifts and feedback effects on their evolution can be neglected. For a detailed study of DM-triggered WD ignition on baryonic feedback, see Ref. [42]. Finally, note that the WD mass fraction, as shown in Fig. S1 [17], indicates that $\sim 80\%$ of the WDs have a mass below $0.9 M_\odot$, well below the Chandrasekhar limit. The detonation of those lower-mass WDs is expected to produce the dimmer Ca-rich events.

Dwarf galaxy model.—The Milky Way is surrounded by smaller structures known as dwarf spheroidal galaxies (dSphs) [43]. While the total stellar population of dSphs pales in comparison to the Milky Way, they may dominate the DM-WD interaction rate due to a concordance of three factors.

First, dSphs contain a significant DM density, with mass-to-light ratios that normally exceed a factor of 100 [43]. Second, the velocity dispersion within dSphs is extremely low, often ~ 10 km s^{-1}. This significantly enhances the DM-WD cross section via gravitational focusing.

Third, dSphs stellar populations are old, increasing the fraction of stars that have evolved off of the main sequence and become WDs. Many dSphs, especially the subpopulation known as ultrafaint dSphs, show evidence for only a single star-formation episode at reionization [44,45]. While larger dSphs, such as Carina, also have later, episodic, star formation [46], they are still biased towards very old stars.

This confluence of factors produces a triggered SN rate in the dSph population that is similar to that expected from the main galaxy, despite significantly smaller star counts. We model the WD population in dSphs using the initial mass function from Ref. [47]:

$$\zeta_{\text{dSh}} = \frac{\kappa}{M^\alpha} \begin{cases} \kappa = 0.11, \alpha = 1.3, & \text{if } \frac{M}{M_\odot} \geq 0.08, \\ \kappa = 1.34, \alpha = 0.3, & \text{if } \frac{M}{M_\odot} < 0.08. \end{cases}\quad(10)$$

We assume that dSphs have a uniform stellar age of 10 Gyr, which produces a larger WD fraction:

$$f_{\text{WD}}^{\text{dSh}} = \frac{\int_{M_\odot}^{8M_\odot} dM \zeta_{\text{dSh}}}{\int_0^{100 M_\odot} dM \zeta_{\text{dSh}}} \approx 0.17.\qquad(11)$$

We adopt a functional form for the stellar density from Ref. [48], and utilize the gNFW DM profile for both a cuspy profile ($\gamma = 1$ with $r_c = 800$ pc) and a cored profile ($\gamma = 0.1$ with $r_c = 150$ pc) (see, e.g., Ref. [49] for a discussion of the core-cusp problem). In dSphs, both the DM velocity dispersion and stellar kinematic profile are determined from kinematic data [48]. Using these profiles, we calculate the triggered SN rate in a dSph with a given halo mass, half-light radius, and stellar mass function using Eq. (2). For example, given the input values for Fornax from Ref. [43], we find an event rate of $(4 \pm 2) \times 10^{-5}$ yr^{-1} given a PBH mass of 10^{24} g. The expected total rate from all MWEG dSphs is about an order of magnitude larger.

Dwarf distributions and properties.—As reported in Ref. [50], state-of-the-art N-body simulations agree with
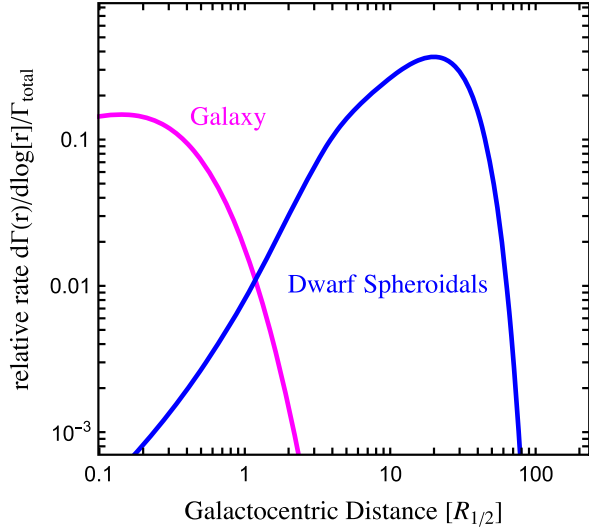
FIG. 2. The modeled relative event rate per unit log distance for triggered SN events stemming from the galaxy and dSphs as a function of the galactocentric distance. The best-fit SN rate from dSphs exceeds the Milky Way signal by a factor of ~2–4.

FIG. 3. The combination of PBH mass and abundance (where f_{DM} represents the fraction of the DM mass composed of PBHs) required to produce a triggered SN rate compatible with Ca-rich transient observations. The 95% C.L. exclusion region from stellar microlensing in M31 by Subaru (HSC) [18,19] is shown as a dashed blue line.

the observed radial and size distribution of MW satellites. Thus, we can use the properties of known MW satellites to extract statistical quantities that represent the MWEG dSph population, comparing our results to the triggered SN rate from the galaxy itself. The radial distribution of dSphs is well described by a modified Gaussian

$$P_r^{dSph}(\mu, \sigma, \alpha) = \left(1 + \mathrm{Erf}\left(\frac{\alpha(r-\mu)}{\sqrt{2}\sigma}\right)\right) \times \exp\left[-\frac{(r-\mu)^2}{2\sigma^2}\right],$$

(12)

where α is a skewness parameter and Erf is the Gaussian error function. The best-fit parameters, based on the MW dwarf sample in Ref. [43] are $\mu = 12$ kpc, $\sigma = 114$ kpc, and $\alpha = 12$. We generate a synthetic sample of dSphs around a galaxy and estimate the total WD ignition rate expected from the dSph population:

$$R_{dSph} \approx (12 \pm 8) \times 10^{-4} \left(\frac{10^{24} \text{ g}}{M_{PBH}}\right) \text{ yr}^{-1},$$

(13)

which implies a ratio R_{dSph}/R_{MW} between 1 and 4. We discuss our synthetic dSph population in the Supplemental Material [17], which contains Ref. [51].

Results.—In Fig. 2 we show the normalized, differential event rate in 1 kpc bins, under the assumption that $R_{dSph} = 2R_{MW}$. The largest signal (by far) is in the galactic outskirts. We compare our results to observations, which include galaxies that differ from the Milky Way, by renormalizing the radial distribution of our model to the half-light radius of each galaxy. We use $R_{1/2} \approx 6$ kpc as a benchmark for the Milky Way. We overlay our theoretical

expectations for the cumulative Ca-rich transient rate with observations from Ref. [2], see Fig. 1. The data is best described with a relative dSph event rate of $R_{dSph} \approx 3R_{MW}$, which falls within our theoretical expectations.

The total event rate of Ca-rich Gap transients was estimated to be $R_{obs}^{total} = 3.19^{+1.45}_{-0.96} \times 10^{-6}$ Mpc^{-3} yr^{-1} [22]. This corresponds to an event rate for an MWEG of $R_{obs}^{Galaxy} = 4 \pm 2 \times 10^{-4}$ yr^{-1}. We note that the event rates in Eqs. (9) and (13) scale inversely with the PBH mass. Moving to smaller PBH masses increases the number of PBHs (and thus the total interaction rate), but also increases the minimum WD mass at which an interaction triggers an SN explosion. As shown in Fig. S1 in [17], PBHs with masses of 10^{24} g can trigger SNe in WDs as small as $0.4M_\odot$. However, WD explosions in such low-mass stars may have a reduced detection probability compared to more massive WDs [14].

In Fig. 3 we show fits for the PBH mass and fractional abundance. The PBH abundance is parametrized as a fraction of the total observed DM abundance [39], $f_{DM} = \Omega_{PBH}/\Omega_{DM}$. Our uncertainty band encompasses the observational and modeling uncertainty in the event rate. This assumes a Ca-rich gap transient detection efficiency calculated by Ref. [2]. We also show the claimed 95% C.L. exclusion region from a 7-h-long dedicated microlensing search in the Andromeda galaxy using the Hyper Suprime-Cam (HSC) on the Subaru telescope [18,19]. The upper limit is based on the detection of a single candidate event, whereas the team expected multiple detections in a PBH dominated DM scenario. Verification of the HSC limits would be highly desirable given our

findings. Other constraints on PBHs in this mass range have been claimed in Refs. [52,53], but Ref. [16] showed that current modeling and astrophysical uncertainties do not support the robustness of those bounds.

If the Ca-rich transient population includes additional, fainter, SNe than considered by Ref. [2], the PBH mass range begins to be squeezed from both sides. High-mass PBHs become more strongly constrained by HSC observations, while low-mass PBH begin to be excluded because they could not detonate very low-mass WDs. Thus, it is intriguing that the expected PBH mass and abundance range agree with the parameters needed to explain recent NANOGrav observations [54].

Discussion and conclusions.—In this Letter, we argue that Ca-rich gap transients may be explained by the ignition of relatively low-mass WDs, triggered by the transition of heavy DM objects. In our minimal scenario, these objects could be PBHs with masses of large asteroids, between $\sim 10^{21}$ and $\sim 10^{24}$ g, and radii of $\sim \mathcal{O}(1)$ nm to $\sim \mathcal{O}(1)$ μm.

Two observations motivate this possibility. First, the Ca-rich transients are faint compared to standard SNIa and have peculiar spectral features that are difficult to model with standard astrophysical models. In the triggered ignition picture, this feature is expected, since the transits of sufficiently heavy ($> 10^{21}$ g) DM can ignite even low-mass WDs, with $M_{\mathrm{WD}} < 0.8 M_\odot$, which produces a fainter detonation signal. As discussed in Supplemental Material [17] those low mass WDs constitute over 80% of the total WD population, leading to the expectation of dimmer signals, identified as Ca-rich transients, being likely in the ignition scenario.

Second, the spatial distribution of Ca-rich transients around a host galaxy differs significantly from the SNIa distribution, see Fig. 1, originating from binary systems involving at least one (heavier) WD. While SNIa events match the stellar distribution of Milky Way-like galaxies, the Ca-rich transients do not. In the context of DM interactions, however, this behavior is explained by the fact that dSphs can dominate the event rate since they contain an old population of WDs embedded in a compact DM halo with low-velocity dispersions. Note that the inner kpc region of the galaxies might have lower sensitivity due to crowding, which would explain the current absence of Ca-rich transient observations near the centers of galaxies.

Observational outlook.—The low luminosity of Ca-rich transients confines their discovery in ongoing surveys to a distance of ~ 150 Mpc. The largest ongoing systematic survey is being carried out by the Zwicky Transient Facility, which classified 8 new events in its first 16 months of operation [22]. The search volume will increase by more than 2 orders of magnitude once the deeper survey at LSST starts in 2024. However, the bottleneck for the identification of Ca-rich transients in the Rubin era will likely be dominated by spectroscopic resources. Hence, a more immediate route to investigate whether Ca-rich transients

originate from DM interactions could be to search for dSphs at the locations of observed Ca-rich transients. For satellite galaxies brighter than $M_{\mathrm{IR}}^{\mathrm{dSh}} \sim -7$ mag, the average absolute magnitude of the known Milky-Way satellites [55], JWST observations could have the sensitivity to resolve dSphs for the current sample of Ca-rich transients [22]. Such an association would strongly probe our scenario.

[*] juri.smirnov@liverpool.ac.uk
[†] ariel@fysik.su.se
[‡] linden@fysik.su.se
[§] edvard@fysik.su.se

[1] H. B. Perets *et al.*, Nature (London) **465**, 322 (2010).
[2] R. Lunnan *et al.*, Astrophys. J. **836**, 60 (2017).
[3] X. Meng and Z. Han, Astron. Astrophys. **573**, A57 (2015).
[4] P. Fayet, D. Hooper, and G. Sigl, Phys. Rev. Lett. **96**, 211302 (2006).
[5] J. Bramante, Phys. Rev. Lett. **115**, 141301 (2015).
[6] J. F. Acevedo and J. Bramante, Phys. Rev. D **100**, 043020 (2019).
[7] H.-S. Chan, M.-c. Chu, S.-C. Leung, and L.-M. Lin, Astrophys. J. **914**, 138 (2021).
[8] E. Witten, Phys. Rev. D **30**, 272 (1984).
[9] J. F. Acevedo, J. Bramante, and A. Goodman, Phys. Rev. D **105**, 023012 (2022).
[10] B. J. Carr, K. Kohri, Y. Sendouda, and J. Yokoyama, Phys. Rev. D **81**, 104019 (2010).
[11] B. Carr, F. Kuhnel, and M. Sandstad, Phys. Rev. D **94**, 083504 (2016).
[12] R. Janish, V. Narayan, and P. Riggins, Phys. Rev. D **100**, 035008 (2019).
[13] H. Steigerwald, D. Rodrigues, S. Profumo, and V. Marra, Mon. Not. R. Astron. Soc. **510**, 4779 (2022).
[14] P. W. Graham, S. Rajendran, and J. Varela, Phys. Rev. D **92**, 063007 (2015).
[15] P. W. Graham, R. Janish, V. Narayan, S. Rajendran, and P. Riggins, Phys. Rev. D **98**, 115027 (2018).
[16] P. Montero-Camacho, X. Fang, G. Vasquez, M. Silva, and C. M. Hirata, J. Cosmol. Astropart. Phys. 08 (2019) 031.
[17] See Supplemental Material at http://link.aps.org/supplemental/10.1103/PhysRevLett.132.151401 for a review of the dark matter-induced white dwarf ignition

mechanism, and our approach to generating synthetic dwarf spheroidal populations.

[18] H. Niikura *et al.*, Nat. Astron. **3**, 524 (2019).

[19] N. Smyth, S. Profumo, S. English, T. Jeltema, K. McKinnon, and P. Guhathakurta, Phys. Rev. D **101**, 063005 (2020).

[20] M. M. Kasliwal *et al.*, Astrophys. J. **755**, 161 (2012).

[21] P. H. Sell, T. J. Maccarone, R. Kotak, C. Knigge, and D. J. Sand, Mon. Not. R. Astron. Soc. **450**, 4198 (2015).

[22] K. De *et al.*, Astrophys. J. **905**, 58 (2020).

[23] A. Polin, P. Nugent, and D. Kasen, Astrophys. J. **906**, 65 (2021).

[24] Y. Zenati, H. B. Perets, L. Dessart, W. V. Jacobson-Gal'an, S. Toonen, and A. Rest, Astrophys. J. **944**, 22 (2023).

[25] P. Asadi, E. D. Kramer, E. Kuflik, G. W. Ridgway, T. R. Slatyer, and J. Smirnov, Phys. Rev. D **104**, 095013 (2021).

[26] P. Asadi, E. D. Kramer, E. Kuflik, G. W. Ridgway, T. R. Slatyer, and J. Smirnov, Phys. Rev. Lett. **127**, 211101 (2021).

[27] C. Gross, G. Landini, A. Strumia, and D. Teresi, J. High Energy Phys. 09 (2021) 033.

[28] M. A. Fedderke, P. W. Graham, and S. Rajendran, Phys. Rev. D **101**, 115021 (2020).

[29] F. Timmes, https://cococubed.com/code_pages/coldwd.shtml (2015).

[30] F. X. Timmes and S. E. Woosley, Astrophys. J. **396**, 649 (1992).

[31] J. Bramante, T. Linden, and Y.-D. Tsai, Phys. Rev. D **97**, 055016 (2018).

[32] J. F. Navarro, C. S. Frenk, and S. D. M. White, Astrophys. J. **462**, 563 (1996).

[33] J. I. Read, J. Phys. G **41**, 063101 (2014).

[34] M. J. Reid, K. M. Menten, A. Brunthaler, X. W. Zheng, T. M. Dame, Y. Xu, J. Li, N. Sakai, Y. Wu, K. Immer, B. Zhang, A. Sanna, L. Moscadelli, K. L. J. Rygl, A. Bartkiewicz, B. Hu, L. H. Quiroga-Nuñez, and H. J. van Langevelde, Astrophys. J. **885**, 131 (2019).

[35] E. V. Karukes, M. Benito, F. Iocco, R. Trotta, and A. Geringer-Sameth, J. Cosmol. Astropart. Phys. 09 (2019) 046.

[36] P. R. Kafle, S. Sharma, G. F. Lewis, and J. Bland-Hawthorn, Astrophys. J. **794**, 59 (2014).

[37] M. Juric *et al.* (SDSS Collaboration), Astrophys. J. **673**, 864 (2008).

[38] A. M. Hopkins and J. F. Beacom, Astrophys. J. **651**, 142 (2006).

[39] N. Aghanim *et al.* (Planck Collaboration), Astron. Astrophys. **641**, A6 (2020); **652**, C4(E) (2021).

[40] P. Kroupa and C. Weidner, Astrophys. J. **598**, 1076 (2003).

[41] K. Nomoto, Astrophys. J. **277**, 791 (1984).

[42] J. F. Acevedo, H. An, Y. Boukhtouchen, J. Bramante, M. Richardson, and L. Sansom, arXiv:2309.08661.

[43] A. W. McConnachie, Astron. J. **144**, 4 (2012).

[44] M. Monelli, S. L. Hidalgo, P. B. Stetson, A. Aparicio, C. Gallart, A. E. Dolphin, A. A. Cole, D. R. Weisz, E. D. Skillman, E. J. Bernard, L. Mayer, J. F. Navarro, S. Cassisi, I. Drozdovsky, and E. Tolstoy, Astrophys. J. **720**, 1225 (2010).

[45] C. Gallart, M. Monelli, L. Mayer, A. Aparicio, G. Battaglia, E. J. Bernard, S. Cassisi, A. A. Cole, A. E. Dolphin, I. Drozdovsky, S. L. Hidalgo, J. F. Navarro, S. Salvadori, E. D. Skillman, P. B. Stetson, and D. R. Weisz, Astrophys. J. Lett. **811**, L18 (2015).

[46] T. J. L. de Boer, E. Tolstoy, B. Lemasle, A. Saha, E. W. Olszewski, M. Mateo, M. J. Irwin, and G. Battaglia, Astron. Astrophys. **572**, A10 (2014).

[47] M. Gennaro, M. Geha, K. Tchernyshyov, T. M. Brown, R. J. Avila, C. Conroy, R. R. Muñoz, J. D. Simon, and J. Tumlinson, Astrophys. J. **863**, 38 (2018).

[48] M. G. Walker, M. Mateo, E. W. Olszewski, J. Penarrubia, N. W. Evans, and G. Gilmore, Astrophys. J. **704**, 1274 (2009); **710**, 886(E) (2010).

[49] P. Boldrini, Galaxies **10**, 5 (2021).

[50] R. J. J. Grand, F. Marinacci, R. Pakmor, C. M. Simpson, A. J. Kelly, F. A. Gómez, A. Jenkins, V. Springel, C. S. Frenk, and S. D. M. White, Mon. Not. R. Astron. Soc. **507**, 4953 (2021).

[51] R. J. J. Grand and S. D. M. White, Mon. Not. R. Astron. Soc. **511**, L55 (2022).

[52] F. Capela, M. Pshirkov, and P. Tinyakov, Phys. Rev. D **87**, 023507 (2013).

[53] G. Defillon, E. Granet, P. Tinyakov, and M. H. G. Tytgat, Phys. Rev. D **90**, 103522 (2014).

[54] V. De Luca, G. Franciolini, and A. Riotto, Phys. Rev. Lett. **126**, 041303 (2021).

[55] J. D. Simon, Annu. Rev. Astron. Astrophys. **57**, 375 (2019).